ELSEVIER

Spectrochimica Acta Part B 63 (2008) 1 – 8

SPECTROCHIMICA ACTA PART B

www.elsevier.com/locate/sab

Review

The prediction of thick target electron bremsstrahlung spectra in the 0.25–50 keV energy range

Jorge Trincavelli, Gustavo Castellano *

Facultad de Matemática, Astronomía y Física, Universidad Nacional de Córdoba. M. Allende s/n, (5016) Ciudad Universitaria, Córdoba, Argentina
Consejo Nacional de Investigaciones Científicas y Técnicas de la República Argentina

Received 1 October 2007; accepted 13 November 2007
Available online 22 November 2007

Abstract

The importance of electron bremsstrahlung has continuously grown since its early discovery more than one century ago, increasingly being involved in different scientific areas. The present work deals with the prediction of thick-target bremsstrahlung spectrum in the frame of scanning electron microprobe analysis. X-ray energies considered range from 0.25 to 50 keV, whereas the models discussed involve electron incident energies up to 50 keV. The main attempts proposed to describe the thick target bremsstrahlung by electron impact are reviewed. Developments carried out from theoretical bases are considered, as well as the role played by Monte Carlo simulations. The results achieved by empirical models are particularly emphasized in view of their reliability in the description of the bremsstrahlung spectrum by means of analytical functions of the atomic number, beam energy and photon energy.

Pacs: 32.30.Rj; 34.80.-I; 41.60.-m; 41.75.Fr
Keywords: Bremsstrahlung; EPMA; Standardless analysis

Contents

1. Introduction

When charged particles traverse matter, several interactions take place, involving directional deflections and energy interchange with the irradiated material, which may in turn give rise to the emission of secondary radiation. Particularly, Coulomb interactions – mainly with atomic nuclei – give rise to the emission of electromagnetic radiation in a continuous range of energies, referred to as bremsstrahlung.

The importance of electron bremsstrahlung has continuously grown since its discovery by Röntgen in 1895 [1–3]. In addition to the intrinsic theoretical interest of this kind of interaction, it has increasingly been involved in different scientific areas. In medical physics, for example, its knowledge is extremely important in the design of appropriate radioisotope shielding materials; linear

* Corresponding author. Facultad de Matemática, Astronomía y Física, Universidad Nacional de Córdoba. M. Allende s/n, (5016) Ciudad Universitaria, Córdoba, Argentina.
E-mail address: gcas@famaf.unc.edu.ar (G. Castellano).

0584-8547/$ - see front matter © 2007 Elsevier B.V. All rights reserved.
doi:10.1016/j.sab.2007.11.009

accelerators used in external radiotherapy require an adequate characterization of photon treatment spectra; and diagnose tools as radiography or more modern computed tomography [4–6] have been possible with the control of sophisticated X-ray tubes. In the frame of materials characterization, X-ray tube spectrum input for quantitative X-ray Fluorescence or related techniques, synchrotron brilliance control or background subtraction in electron probe spectra, are fundamental tools which depend on a reliable description of bremsstrahlung emission. Other interesting examples evidencing the importance of bremsstrahlung prediction are the description of electron energy distributions in plasmas [7] or electron bursts in upper atmosphere [8].

When the irradiated target is thin enough, the emitted spectrum is closely related to the concept of bremsstrahlung cross-section. After the pioneering work of Kulenkampff [9], several measurements were carried out in order to obtain absolute [10–12] or relative [13–16] determinations of differential electron bremsstrahlung cross-sections in this kind of targets. Similar experiments were also performed in gas samples [17–21]. Many of these experimental values have been used to check theoretical models for cross-sections [22–33], as subsequently reviewed by Koch and Motz [34], Acosta [35] and Quarles and Portillo [36].

On the other hand, when the irradiated target is thicker, the convolution of the different possible interactions inhibits the straightforward obtention of an analytical expression for the corresponding bremsstrahlung spectrum. The description of this photon distribution has drawn the attention of different research areas, since the adequate knowledge of the emitted spectrum may be used for different purposes: X-ray tube spectrum input for quantitative X-Ray Fluorescence or related techniques, background subtraction in x-ray spectra induced by electron impact [37], standardless quantitative electron probe microanalysis (EPMA) for particles [38] or bulk samples [39], etc.

The present work aims to provide a review of the prediction of thick-target bremsstrahlung spectra in the frame of scanning electron microprobe analysis, i.e., for X-ray energies ranging from 0.25 to 50 keV corresponding to electron incident energies up to 50 keV. It is worth mentioning that the available models in the literature usually deal with normal incidence, since this is the most frequently used geometrical arrangement in electron-probe experiments. The models presented below for bremsstrahlung description are intended to this experimental configuration, unless explicitly indicated.

2. Theoretical developments

Spectra recorded in an electron microprobe consist of characteristic peaks superimposed upon a continuum spectrum ranging from very low energies up to the incidence energy E_o, basically the bremsstrahlung spectrum. An adequate description of this continuum spectrum is of great interest in microanalysis, since an incorrect subtraction of this background may lead to important experimental errors.

Several approaches have been proposed for predicting the bremsstrahlung spectrum. Theoretical models are based in the assessment of a numerical integration involving the bremsstrahlung differential cross-section Q for the emission of a photon of energy E and the stopping power S as a function of the electron energy E':

$$I = \frac{N_A}{A}\int_{E_o}^{E}\frac{Q}{S}\mathrm{d}E', \tag{1}$$

where N_A is Avogadro's number and A is the atomic weight. Absorption correction and backscattering losses may be taken into account separately, or incorporated into the integrand.

The well-known expression developed by Kramers in 1923 [40] is based on a classical approximation in the calculation of the bremsstrahlung cross-section and the Thomson–Whiddington law [41] for the stopping power. His expression agrees with the empirical formula obtained previously by Kulenkampff [9], for which Dyson [42] fitted the corresponding overall constant. Since this model simply accumulates the contribution corresponding to successive thin targets conforming a thick sample, corrections must be applied to account for backscatter losses and photon absorption in order to enable comparison with experimental spectra. According to this description, the total intensity (number of photons per unit time) detected per incident electron with energies between E and $E+\Delta E$ when a sample of atomic number Z is irradiated with electrons of energy E_o can be expressed as:

$$\Delta I = GZ\frac{E_o - E}{E}\Delta E,$$

where the factor G involves the sample absorption to the observed radiation, the losses due to backscattering of electrons, the detection efficiency to energy E and the solid angle fraction subtended by the detector.

Storm [43] carried out the assessment of Eq. (1) for the particular case of tungsten, by using Kirkpatrick–Wiedmann cross-sections [24] based on Sommerfeld formalism [22]. He also compared with non-relativistic [44] and relativistic [45–47] approaches based on Born-approximation. Bethe stopping power [48] tabulated by Berger and Seltzer [49] was used, whereas backscattering losses were taken into account by including an additional factor in the integrand. Photon attenuation was also included in the numerical integral above. The electron energies considered ranged from 12 to 300 keV.

Rao-Sahib and Wittry [50] modified the bremsstrahlung cross-sections of Kirkpatrick–Wiedmann, in order to achieve better agreement with the original Sommerfeld equation. In addition, they performed a parabolic extrapolation for the amendment of Bethe's stopping power at low electron energies. Corrections for electron backscattering were carried out according to Duncumb and Reed's [51] energy distribution of backscattered electrons. Although these authors did not arrived to an analytical expression, their work was used as the basis for subsequent developments. For instance, Reed [52] used their expressions for backscattering losses and their modified Bethe's law for the stopping power. He performed Monte Carlo simulations in order to achieve an improved assessment of a separate absorption correction for the continuum emission. Using results obtained for Al, Cu, Ag

and Au, he obtained an expression which appears as a slight modification to Kramers–Kulenkampff formula:

$$\Delta I = GZ\frac{E_o - E}{E^{1+a}}\Delta E. \quad (2)$$

where a is a constant optimized only for Z ranging from 13 to 29, and E_o from 15 to 20 keV. In the procedure followed to achieve this expression, Philibert's depth distribution [53] was adopted for bremsstrahlung emission in order to perform the corresponding absorption correction:

$$f(\chi) = \frac{1}{\left(1+\frac{\chi}{\sigma}\right)\left(1+\frac{h}{1+h}\frac{\chi}{\sigma}\right)},$$

where $\chi=\mu$ csc ψ, μ being the mass-absorption coefficient for energy E and ψ, the take-off angle, $h=1.2A/Z^2$ and

$$\sigma = \frac{4\cdot 10^5}{E_o^{1.65} - E^{1.65}}$$

involves the photon energy E instead of the binding energy corresponding to characteristic emission, as originally proposed by Philibert.

A similar work was performed recently by Ambrose et al. [54], and later applied by Semaan and Quarles [55] to describe continuum spectra from a scanning electron microscope. The novelty of this approach is the inclusion of the more realistic partial-wave relativistic cross-sections given by Kissel et al [31]. Bethe stopping power tabulated by Berger and Seltzer [56] is used, and backscattering losses extending Storm's approach for tungsten to other atomic numbers, by using backscattering coefficient suggested by August and Wernisch [57]. Semaan and Quarles claim a good agreement with experimental data, although they normalize for each atomic number in the comparisons performed. On the other hand, no analytical expression is suggested for spectrum prediction.

3. Monte Carlo simulations

Complete spectra originated in an electron microprobe have also been obtained from Monte Carlo simulations, an alternative which began in a number of early articles (see e.g. Messel et al. [58], Zerby and Moran [59], Berger and Seltzer [60] or Jenkins et al. [61]). Although recent attempts have involved reliable cross-section models and modern numerical algorithms [62–64], few efforts have been addressed to achieve an analytical expression for the prediction of the bremsstrahlung spectrum. To this aim, Statham [65] performed Monte Carlo simulations to study the continuum absorption correction and the effects of anisotropy in the emission of bremsstrahlung. His results have been included as a modification to Reed's expression as:

$$\Delta I = GZ\frac{E_o - E}{E^{1+a+b}}\Delta E, \quad (3)$$

where the additional exponent b accounts for the emission anisotropy, which is reflected in the dependence on both incident and take-off angles. These two exponents were determined with a 20 keV electron beam for five elements (Al, Ti, Mn, Cu, Au), and two geometrical arrangements: normal incidence and take-off angle of 40°, and 45°–45° geometry.

4. Empirical models

Kramers model has largely been used as a basis for modeling X-ray tube emission spectra [66–69], where the most important region corresponds to energies greater than, say, 5 keV due to the strong attenuation of low energies in the tube window. Nevertheless, this kind of models is not suitable in EPMA, since even when conventional detectors are used, the thickness of the windows involved in the detection process is much smaller than that of X-ray tubes, allowing to record photons of energies down to 1 keV. For this reason, a number of empirical modifications, mainly for normal incidence, have been suggested to improve the description of the bremsstrahlung spectrum in EPMA.

In 1974 Lifshin [70] suggested a modification to Kramers law, incorporating an empirical degree of freedom by means of a quadratic term:

$$\Delta I = GZ\frac{E_o - E}{E}[1 + c(E_o - E)]\Delta E, \quad (4)$$

where c is a fitting parameter.

Fiori et al. [71] used Lifshin's expression to perform background subtraction in energy dispersive EPMA. They suggested to fit the involved constants by means of considering two different energies in the continuum spectrum for which there are no characteristic photons.

Whilst Eqs. (2), (3) and (4) may be adequate to carry out a correct background subtraction in experimental spectra, they are not useful to predict spectra as a function of Z, E_o and E. Since such a prediction is a basic requirement for different standardless analysis approaches [38,72], the expressions dependent on empirical parameters are not of interest in this context: the information desired is hidden precisely within these parameters.

Several authors tried to find analytical expressions for the continuum background so that only one parameter remained undetermined [73–77]. This scaling factor depends on the particular detection geometry and must be fitted for each equipment — but not for each spectrum because it is not related neither to the sample composition nor to the excitation conditions.

Smith et al. [73] obtained an analytical expression for the continuum spectrum as a function of Z, E y E_o following a previous development performed by Rao-Sahib and Wittry [78]:

$$\Delta I = G\left(\frac{E_o - E}{E}\right)^x Z^n \Delta E,$$

where

$$n = E\cdot(0.0739 - 0.0051\ln Z) + 1.6561 - 0.115\ln Z,$$
$$x = 1.76 - 0.00145Z/E.$$

Small et al. [74] observed that discrepancies between the existent models for bremsstrahlung and experimental values

were about 50% or even 100%. For this reason they developed an expression by fitting a large set of experimental data:

$$\Delta I = G\left(Z\frac{E_o - E}{E}\right)^M e^B \Delta E, \tag{5}$$

where

$$M = 0.00599E_o + 1.05,$$
$$B = -0.0322E_o.$$

Nevertheless, in a previous work [75] it was pointed out that the predictions given by Eq. (5) were not accurate enough for a wide range of experimental conditions, particularly for high atomic numbers. For this reason, Kramers expression was modified after fitting 52 spectra from targets of diverse composition at several incident energies. The absorption correction used was based on the ionization depth distribution function given by Packwood and Brown [79] with coefficients modified by Riveros et al. [80]. Mass absorption coefficients were calculated with the expression given by Heinrich [81]. This approach involves the assumption of considering the depth distribution of continuum x-ray production similar to that of characteristic radiation, as also considered in previous predictions [73,74]. Although characteristic radiation is isotropically emitted, this is a reasonable approximation: even when each bremsstrahlung photon preferably follows the forward electron direction (particularly for high energies), after a few interactions the electron path looses correlation with the incidence direction. Backscattering losses were accounted for according to the expression given by Statham [82]. This model is a function of the backscattering correction for characteristic photons, for which the model by Love et al. [83] was chosen. Detection efficiency corrections were also taken into account, finally achieving the following expression for bremsstrahlung intensity:

$$\Delta I = G\sqrt{Z\frac{E_o - E}{E}}\times \left(-54.86 - 1.072E + 0.2835E_o + 30.4\ln Z + \frac{875}{Z^2E_o^{0.08}}\right)\Delta E. \tag{6}$$

When dealing with multielemental targets, the compositional dependence of the bremsstrahlung spectrum should be introduced in the elementary equations, rather than artificially substituting Z by the mean atomic number $\overline{Z} = \sum C_j Z_j$ in the final equation [84], C_j being the mass concentration of the jth element. However, as this effect influences spectrum predictions very weakly, the use of $\overline{Z}$ results a very good approximation.

The function obtained describes adequately the continuum x-ray spectrum for electron beam energies ranging from 5 to 35 keV and atomic numbers covering elements from boron to bismuth, including also multielemental samples. Since a Si(Li) detector with a conventional Be window was used for X-ray spectra acquisition, only photon energies above 1 keV were considered, restricting the validity of the model to this energy range. As shown in Fig. 1, the developed expression agrees with measured spectra much closer than the previous model given by Small et al. [74]. It must be emphasized that all comparisons were performed by improving the correction models (absorption and backscattering) included in the factor G of Eq. (5), which indeed produces better results than those of their original work [75].

Comparisons with other models were carried out using a set of spectra larger than that involved in the fitting procedure. In order to provide a figure of merit for the performance of each model, the parameter χ^2 was used to compare the predicted intensities $\tilde{I}$ with the experimental ones I:

$$\chi^2 = \frac{1}{N}\sum_{i=1}^{N}\frac{\left(I_i - \tilde{I}_i\right)^2}{\tilde{I}_i},$$

where i denotes each of the N channels in the considered spectrum. With the aim of obtaining a global value of χ^2 for the whole set of spectra, an average must be assessed, weighting each χ^2 with the number of channels of the corresponding spectrum. The results are shown in Table 1. It can be seen that the model corresponding to Eq. (6) has a better performance than the others, even in the subset S containing only those elements for which Statham [65] assessed the exponents of Eq. (3).

A similar approach was attempted by Duncumb et al [76], who aimed to provide a method for predicting bremsstrahlung and characteristic intensities for the whole spectrum registered in an electron microprobe. To this end, a large set of experimental spectra (309) was considered to develop and test the model proposed, including a number of measurements registered with detectors sealed with ultra-thin polymer windows. The resulting formula was

$$\Delta I = GZF(Z, E_o)\left(\frac{E_o - E}{E}\right)^{P(Z)}. \tag{7}$$

No final expressions were given for the functions F and P, since the authors stated that an optimization process was still required. They only gave values for a few particular cases: three elements and four incident energies. A comparison with previous models was shown for only one of these cases, suggesting that their prediction achieved better agreement with experimental data. Nevertheless, the restriction of the model to specific situations inhibits the use of Eq. (7) for arbitrary samples.

In addition, an important remark must be done regarding the thin-window detector efficiency. Since polymer films are supported on silicon grids, the authors suggest that for low energies the corresponding shadowing effect may be accounted for by a reduction of the solid angle subtended by the detector, whereas for energies greater than 10 keV, this obscuration may be ignored [76,85]. No special care was taken for the transition energy region, pointing that peak-to-background ratios are unaffected by this shadowing effect, although the bremsstrahlung spectrum may be strongly distorted if the detector efficiency is not accurately assessed for the whole energy range. In fact, inaccuracies in the

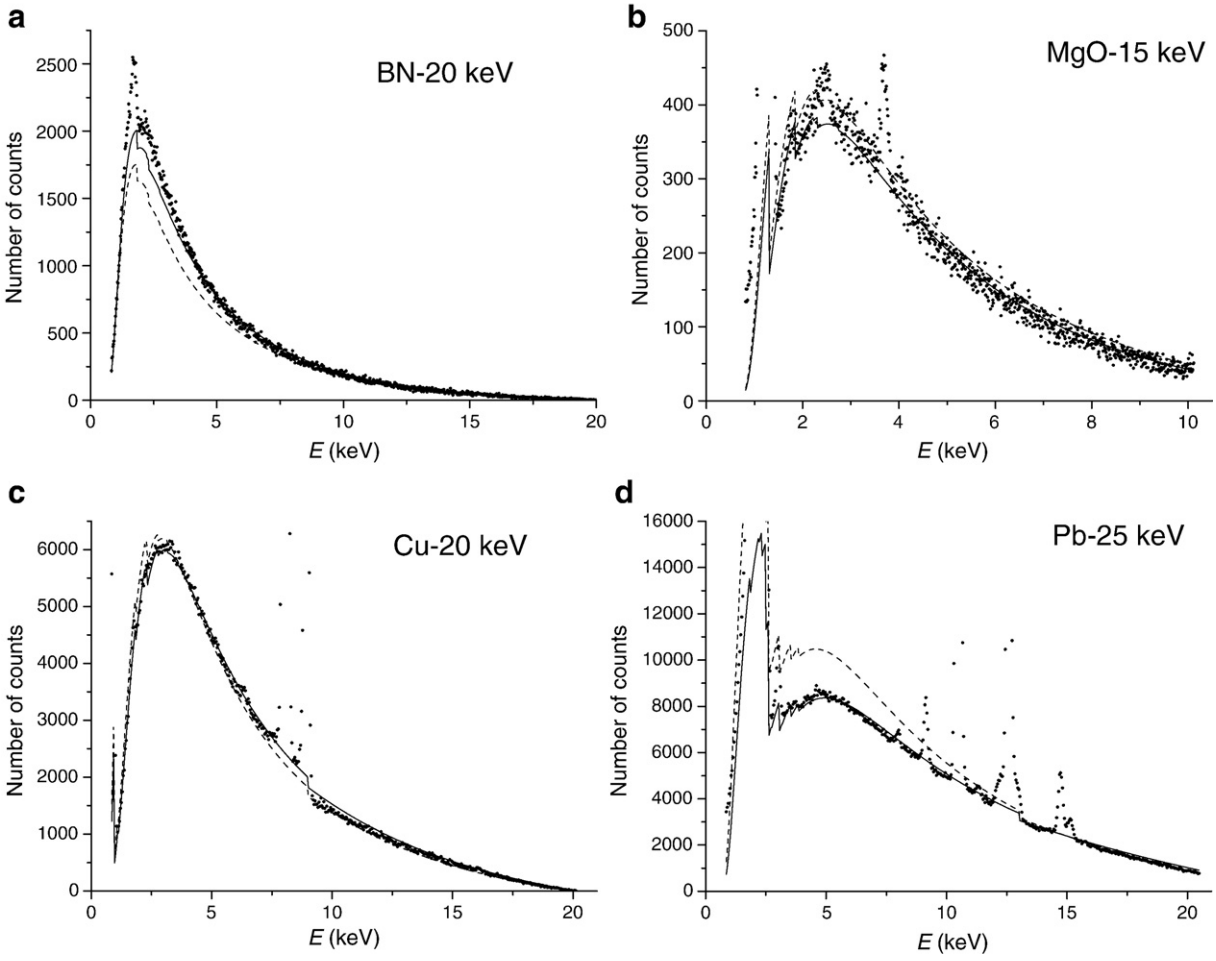

Fig. 1. Prediction of spectra for standard samples. Experimental: dots; Small et al. [74]: dashed line; Trincavelli et al. [75]: solid line.

description of the detector efficiency are transferred to the background modeling.

A description of the ultra-thin window detector efficiency for the whole energy range may be achieved from elementary considerations. If the attenuations in the involved layers (even in the silicon supporting grid) are properly accounted for, an analytical expression may be obtained [86], which is plotted in Fig. 2. As can be seen, the transition energy region for the particular detector geometry must be adequately described.

Spectra registered with a thin-window detector were also considered in a subsequent work [77]. A large set of spectra was involved in the fitting process in order to achieve a reliable

Table 1
Global χ^2 values for the comparison performed by Trincavelli et al. [75]. Reed's model [52] with coefficients given by Statham [65] and the expression given by Small et al. [74] were also assessed

X^2	Subset S	Whole set
	(6015 data)	(35361 data)
Trincavelli et al.	4.3	4.1
Reed-Statham	9.9	–
Small et al.	97	65

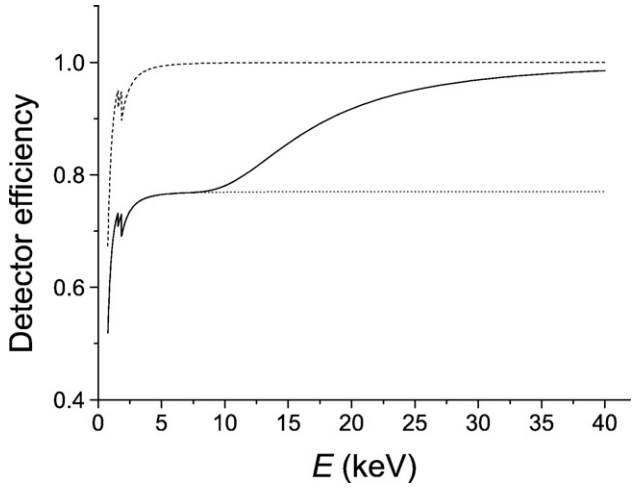

Fig. 2. SUTW Sapphire Si(Li) detector efficiency. The crystal front area is 10 mm^2 and the ultra-thin window is a Moxtek AP3.3 supported by a 380 μm thick silicon grid, 77% open area. Solid line: real efficiency; dotted line: underestimate for infinite silicon thickness (full shadowing effect); dashed line: overestimate by ignoring the effect of the silicon structure.

expression for the continuum function which describes properly the bremsstrahlung spectrum for photon energies ranging from 0.25 to 20 keV and atomic numbers between 4 and 83, at beam energies ranging from 5 to 38 keV. The expression obtained in this work is

$$\Delta I = G\sqrt{Z}\frac{E_o - E}{E}\left(-73.90 - 1.2446E + 36.502\ln Z + \frac{148.5E_o^{0.1293}}{Z}\right)\times\left[1 + (-0.006624 + 0.0002906E_o)\frac{Z}{E}\right]\Delta E. \quad (8)$$

Fig. 3 shows a comparison between experimental data and the model of Eq. (8); for the graphs corresponding to pure gold and copper, the model (7) of Duncumb et al. is also displayed. It can be seen that the model corresponding to Eq. (8) has a very good performance. The global χ^2 value for 132 spectra was 5.9 for this model and 29 in the case of the model by Small et al. [74]. The expression of Duncumb et al. only could be assessed for 7 spectra from the whole set, in view of the aforementioned restriction in atomic numbers and beam energies, resulting in a χ^2 value of 73. In the case of the comparison for gold, the curve assessed following this expression exhibits a rather different performance as compared to the corresponding plot given in the original paper; this may be due either to the efficiency prediction these authors gave for the ultra-thin window detector, as mentioned above, or to the low statistics in the spectra used in their fitting procedure.

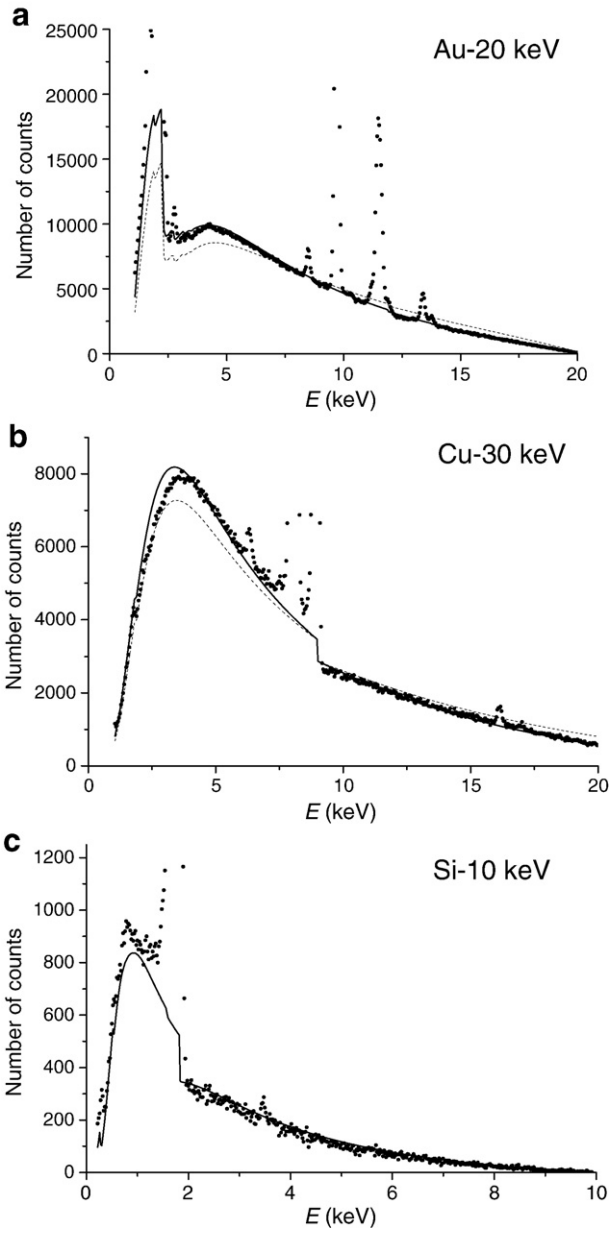

Fig. 3. Prediction of spectra for standard samples. Experimental: dots; Duncumb et al. [76]: dashed line; Castellano et al. [77]: solid line.

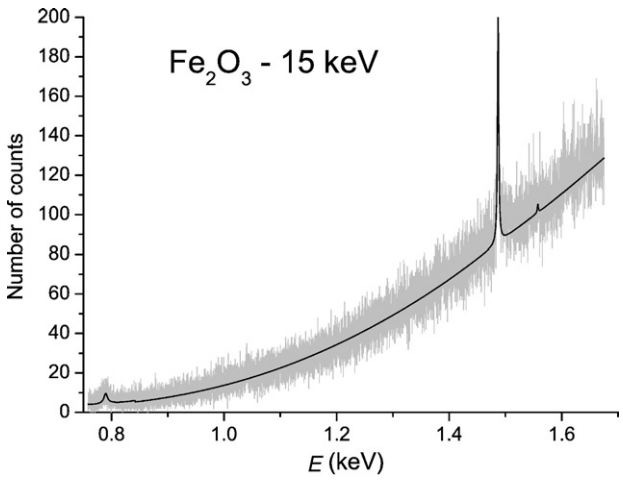

Fig. 4. Prediction of a WDS hematite spectrum irradiated at 15 keV. Experimental: gray line; Eq. (8): black line.

Although the expression (8) has been developed for spectra acquired with energy dispersive systems (EDS) and atomic numbers lower than 84, several attempts have been done to apply the algorithm for describing different situations. An example of a haematite standard spectrum measured with a wavelength dispersive system (WDS) using a TAP crystal at 15 keV

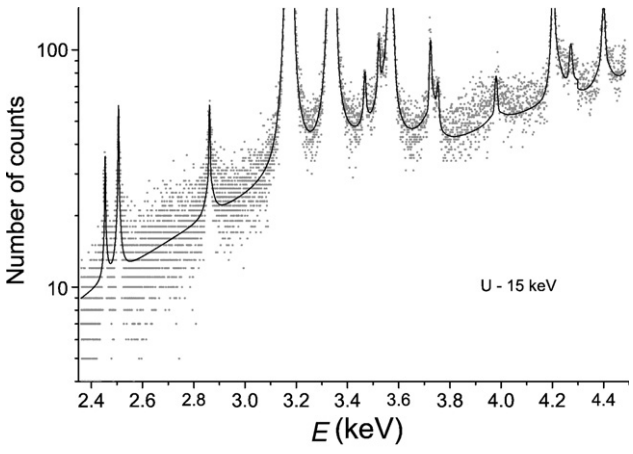

Fig. 5. Prediction of a WDS pure uranium spectrum irradiated at 15 keV. Experimental: dots; Eq. (8): solid line.

is shown [86] in Fig. 4. As usual, a correction for detection efficiency has been carried out, although in this case it is much more important than for EDS spectra; moreover, this correction is the main cause for the background shape displayed.

As a complementary example, Fig. 5 shows another WDS spectrum, registered for a pure uranium standard at 15 keV [87] with a PET crystal. Although the atomic number of the irradiated sample (92) lies outside the range for which the model was originally developed, it can be seen that the agreement is also very good in this case.

5. Conclusion

Several approaches may be faced in order to achieve an appropriate description of the bremsstrahlung spectrum in EPMA. At present, only empirical models have succeeded to provide analytical expressions for the prediction of the continuum spectrum as a function of the atomic number, incident energy and photon energy in a wide range of experimental situations. Further developments based on theoretical considerations will permit a reliable study on the generated bremsstrahlung spectrum — avoiding inaccuracies inherent to backscattering, absorption and efficiency corrections. Recent advances in the Monte Carlo methodology appear as a promising tool to perform "controlled experiments", allowing an appropriate description of the different corrections applied.

Although some examples have been shown for the prediction of wavelength dispersive spectra, a systematic study for this kind of spectrometer is lacking. Even when the bremsstrahlung spectrum is the same, no matter which spectrometer is used, certain aspects must be considered quite differently, particularly the detector efficiency: this parameter may change over an order of magnitude along the energy range covered by a typical crystal.

In addition to the theoretical interest inherent to the knowledge of the bremsstrahlung emission, the most important advantage of having a realistic analytical model for continuum prediction in EPMA is the possibility of improving the performance of standardless quantification methods.

References

[1] W. Röntgen, Eine neue Art von Strahlen, Sitzungsberichten der Würzburger Physik-medic, Gesellschaft, Stahel, Würzburg, 1895.
[2] W. Röntgen, Eine neue Art von Strahlen, II. Mittheilung, Sitzungsberichten der Würzburger Physikal-medic, Gesellschaft, Stahel, Würzburg, 1896.
[3] W. Röntgen, On a new kind of rays, Nature 53 (1369) (January 23, 1896) London.
[4] A. Cormack, Representation of a function by its line integrals, with some radiological applications, J. Appl. Phys. 34 (1963) 2722–2727.
[5] G. Hounsfield, Computerised transverse axial scanning (tomography). Part I. Description of system 1973. Br. J. Radiol. 68 (1995) H166–H172.
[6] W. Kalender, X-ray computed tomography, Phys. Med. Biol. 51 (2006) R29–R43.
[7] M. Lamoureux, P. Charles, General deconvolution of thin-target and thick-target Bremsstrahlung spectra to determine electron energy distributions, Rad. Phys. Chem. 75 (2006) 1220–1231.
[8] D. Smith, L. Lopez, R. Lin, C. Barrington-Leigh, Terrestrial Gamma-Ray Flashes Observed up to 20 MeV, Science 307 (5712) (2005) 1085–1088.
[9] H. Kulenkampff, Über das kontinuierliche Röntgenspektrum, Ann. Phys. 69 (1922) 548–596.
[10] J. Motz, R. Placious, Bremsstrahlung cross-section measurements for 50-kev electrons, Phys. Rev. 109 (1958) 235–242.
[11] D. Rester, N. Edmonson, Q. Peasley, Bremsstrahlung cross sections for Al and Au for incident-electron energies of 0.05 and 0.20 MeV, Phys. Rev. A 2 (1970) 2190–2196.
[12] J. Faulk, C. Quarles, Coincidence measurement of the fully differential cross section for atomic-field bremsstrahlung, Phys. Rev. A 9 (1974) 732–742.
[13] C. Quarles, D. Heroy, Atomic-field bremsstrahlung from 50–140 keV electrons, Phys. Rev. A 24 (1981) 48–54.
[14] R. Ambrose, J. Altman, C. Quarles, Atomic-field bremsstrahlung cross sections for incident electron energy from 50 to 100 keV for atomic numbers from 6 to 92, Phys. Rev. A 35 (1987) 529–539.
[15] V. Ambrose, C. Quarles, R. Ambrose, Thin-target bremsstrahlung at 01 from 50 keV electrons, Nucl. Instrum. Methods Phys. Res. B 124 (1997) 457–463.
[16] C. Quarles, S. Portillo, Looking for polarization bremsstrahlung in the midst of inner-shell ionization: analysis of the X-ray spectrum in electron interactions with thin-film targets, in: J.L. Duggan, I.L. Morgan (Eds.), CP475 Applications of Accelerators in Research and Industry, 1999, pp. 174–177.
[17] R. Hippler, K. Saeed, I. McGregor, H. Kleinpoppen, Z dependence of bremsstrahlung radiation from free atoms, Phys. Rev. Lett. 46 (1981) 1622.
[18] M. Semaan, C. Quarles, Bremsstrahlung spectrum from low-energy electron bombardment of rare gas atoms, Phys. Rev. A 24 (1981) 2280.
[19] M. Semaan, C. Quarles, Z dependence of atomic-field bremsstrahlung, Phys. Rev. A 26 (1982) 3152.
[20] L. Estep, C. Quarles, Atomic-field bremsstrahlung from hydrogen, helium, nitrogen and neon from 5 to 15 keV, Physica B+C 145 (1987) 369–376.
[21] S. Portillo, C. Quarles, Absolute doubly differential cross sections for electron bremsstrahlung from rare gas atoms at 28 and 50 keV, Phys. Rev. Lett. 91 (2003) 173201.
[22] A. Sommerfeld, The deflection and slowing down of electrons, Ann. Phys. 11 (1931) 257–330.
[23] H. Bethe, W. Heitler, On the stopping of fast particles and on the creation of positive electrons, Proc. Roy. Soc. Lond. A 146 (1934) 83–112.
[24] P. Kirkpatrick, L. Wiedmann, Theoretical continuous X-ray energy and polarization, Phys. Rev. 67 (1945) 321–339.
[25] J. Motz, H. Olsen, H. Koch, Electron scattering without atomic or nuclear excitation, Rev. Mod. Phys. 36 (1964) 881–928.
[26] G. Elwert, E. Haug, Calculation of Bremsstrahlung Cross Sections with Sommerfeld–Maue Eigenfunctions, Phys. Rev. 183 (1969) 90–105.
[27] H. Brysk, C. Zerby, S. Penny, Bremsstrahlung cross sections at moderate energies, Phys. Rev. 180 (1969) 104–111.
[28] H. Tseng, R. Pratt, Exact screened calculations of atomic-field bremsstrahlung, Phys. Rev. A 3 (1971) 100–115.
[29] H. Tseng, R. Pratt, Electron bremsstrahlung from neutral atoms, Phys. Rev. Lett. 33 (1974) 516–518.
[30] C. Lee, L. Kissel, R. Pratt, H. Tseng, Electron bremsstrahlung spectrum, 1–500 keV, Phys. Rev. A 13 (1976) 1714–1727.
[31] L. Kissel, C. Quarles, R. Pratt, Shape functions for atomic-field bremsstrahlung from electrons of kinetic energy 1–500 keV on selected neutral atoms $1 \le Z \le 92$, At. Data Nucl. Data Tables 28 (1983) 381–460.
[32] S. Seltzer, M. Berger, Bremsstrahlung spectra from electron interactions with screened atomic nuclei and orbital electrons, Nucl. Instrum. Methods Phys. Res. B 12 (1985) 95–134.
[33] H. Tseng, Relativistic calculations of an elementary process of electron bremsstrahlung from atoms, J. Phys., B At. Mol. Opt. Phys. 30 (1997) L317–L321.
[34] H. Koch, J. Motz, Bremsstrahlung cross-section formulas and related data, Rev. Mod. Phys. 31 (1959) 920–955.
[35] E. Acosta, Cross sections for ionization and bremsstrahlung emission for electrons between 1 and 100 keV. Application to the generation of X-ray spectra, Doctoral Thesis, Universidad Nacional de Córdoba (Córdoba, Argentina), 1997.
[36] C. Quarles, S. Portillo, Review of absolute doubly differential cross-section experiments and cross-section ratios for electron bremsstrahlung from rare gas atom and thin-film targets, Rad. Phys. Chem. 75 (2006) 1187–1200.

[37] S. Reed, Electron Microprobe Analysis, 2nd ed., Cambridge University Press, Cambridge, 1993, pp. 169–173.
[38] J. Trincavelli, R. Van Grieken, Peak-to-background method for standardless electron microprobe analysis of particles, X-Ray Spectrom. 23 (1994) 254–260.
[39] R. Bonetto, G. Castellano, J. Trincavelli, Optimization of parameters in electron probe microanalysis, X-Ray Spectrom. 30 (2001) 313–319.
[40] H. Kramers, On the theory of X-ray absorption and the continuous X-ray spectrum, Phila. Mag. 46 (1923) 836.
[41] R. Whiddington, The transmission of cathode rays through matter, Proc. R. Soc. A 86 (1912) 360–370.
[42] N. Dyson, The continuous X-ray spectrum form electron opaque targets, Proc. Phys. Soc. (London) 73 (1959) 924–936.
[43] E. Storm, Calculated bremsstrahlung spectra from thick tungsten targets, Phys. Rev. A 5 (1972) 2328–2338.
[44] W. Heitler, The quantum theory of radiation, 3rd. ed.Oxford University Press, London, 1954.
[45] H. Bethe, W. Heitler, On the stopping of fast particles and on the creation of positive electrons, Proc. R. Soc. London A146 (1934) 83–112.
[46] F. Sauter, Über den atomaren Photoeffekt in der K-Schale nach der relativistischen Wellenmechanik Diracs, Ann. Phys. 11 (1931) 454–488.
[47] R. Gluckstern, M. Hull Jr., Polarization dependence of the integrated bremsstrahlung cross section, Phys. Rev. 90 (1953) 1030–1035.
[48] H. Bethe, Zur Theorie des Durchgangs schneller Korpuskularstrahlen durch Materie, Ann. Phys. 5 (1930) 325–400.
[49] M. Berger, S. Seltzer, Natl. Acad. Sci. Natl. Res. Council Nucl. Sci. Ser. 39 (1964) 205–268.
[50] T. Rao-Sahib, D. Wittry, X-ray continuum from thick elemental targets for 10–50 keV electrons, J. Appl. Phys. 45 (1974) 5060–5068.
[51] P. Duncumb, S. Reed, Quantitative electron probe microanalysis, in: K. Heinrich (Ed.), Natl. Bur. Stand. Spec. Publ., vol. 298, US Dept. Commerce, Washington, 1968, pp. 133–154.
[52] S. Reed, The shape of the continuous X-ray spectrum and background corrections for energy-dispersive electron microprobe analysis, X-ray Spectrom. 4 (1975) 14–17.
[53] J. Philibert, in: H. Pattee, V. Cosslett, A. Engström (Eds.), X-Ray Optics and X-Ray Microanalysis, Third International Symposium, Stanford, Academic Press, New York, 1963, p. 379.
[54] R. Ambrose, D. Kahler, H. Lehtihet, C. Quarles, Angular dependence of thick-target bremsstrahlung, Nucl. Instrum. Methods Phys. Res., B 56 (1993) 327–329.
[55] M. Semaan, C. Quarles, A model for low energy thick-target bremsstrahlung produced in a scanning electron microscope, X-ray Spectrom. 30 (2001) 37–43.
[56] M. Berger, S. Seltzer, U.S. National Aeronautics and Space Administration Report No. NASA-SP3012 (1964). Current tabulation on the Web: Program ESTAR, http://physics.nist.gov/PhysRefData/Star/Text/ESTAR.html (2000).
[57] H. August, J. Wernisch, Analytical expressions for the electron backscattering coefficient, J. Phys. Status Solidi A 114 (1989) 629–633.
[58] H. Messel, A. Smirnov, A. Varfolomeev, D. Crawford, J. Butcher, Radial and angular distributions of electrons in electron–photon showers in lead and in emulsion absorbers, Nucl. Phys. 39 (1962) 1–88.
[59] C. Zerby, H. Moran, Studies of the longitudinal development of electron–photon cascade showers, J. Appl. Phys. 34 (1963) 2445–2457.
[60] M. Berger, S. Seltzer, Bremsstrahlung and photoneutrons from thick tungsten and tantalum targets, Phys. Res. C 2 (1970) 621–631.
[61] T. Jenkins, W. Nelson, A. Rindi (Eds.), Monte Carlo transport of electrons and photons, Plenum, New York, 1988.
[62] E. Acosta, X. Llovet, F. Salvat, Monte Carlo simulation of bremsstrahlung emission by electrons, Appl. Phys. Lett. 80 (2002) 3228–3230.
[63] F. Salvat, J.M. Fernández-Varea, J. Sempau, X. Llovet, Monte Carlo simulation of bremsstrahlung emission by electrons, Rad. Phys. Chem. 75 (2006) 1201–1219.
[64] D. Roet, C. Ceballos, P. Van Espen, Comparison between MCNP and PENELOPE for the simulation of X-ray spectra in electron microscopy in the keV range, Nucl. Instrum. Methods Phys. Res. B 251 (2006) 317–325.
[65] P. Statham, The generation, absorption and anisotropy of thick-target bremsstrahlung and implications for quantitative energy dispersive analysis, X-Ray Spectrom. 5 (1976) 154–168.
[66] M. Brunetto, J. Riveros, A modification of the Kramers law for the X-ray continuum from thick targets, X-Ray Spectrom. 13 (1984) 60–63.
[67] P. Pella, L. Feng, J. Small, An analytical algorithm for calculation of spectral distributions of X-ray tubes for quantitative X-ray fluorescence analysis, X-Ray Spectrom. 14 (1985) 125–135.
[68] B. Schossmann, H. Wiederschwinger, H. Ebel, J. Wernisch, Comparison of various descriptions of X-ray tube spectra, Adv. X-Ray Anal. 39 (1997) 127–135.
[69] H. Ebel, X-ray tube spectra, X-Ray Spectrom. 28 (1999) 255–266.
[70] E. Lifshin, The use of solid state X-ray detectors for obtaining fundamental X-ray data, Proc. 9th Annual Conf. Microbeam Analysis Society, Ottawa, Canada, 1974, #53.
[71] C. Fiori, R. Myklebust, K. Heinrich, H. Yakowitz, Prediction of continuum intensity in energy-dispersive X-ray microanalysis, Anal. Chem. 48 (1976) 172–176.
[72] J. Trincavelli, G. Castellano, R. Bonetto, L-shell transition rates for Ba, Ta, W, Pt, Pb and Bi using electron microprobe, Spectrochim. Acta Part B 57 (2002) 919–928.
[73] D. Smith, C. Gold, D. Tomlinson, The atomic number dependence of the X-ray continuum intensity and the practical calculation of background in energy dispersive electron microprobe analysis, X-Ray Spectrom. 4 (1975) 149–156.
[74] J. Small, S. Leigh, D. Newbury, R. Myklebust, Modeling of the bremsstrahlung radiation produced in pure-element targets by 10–40 keV electrons, J. Appl. Phys. 61 (1987) 459–469.
[75] J. Trincavelli, G. Castellano, J. Riveros, Model for the bremsstrahlung spectrum in EPMA. Application to standardless quantification, X-Ray Spectrom. 27 (1998) 81–86.
[76] P. Duncumb, I. Barkshire, P. Statham, Improved X-ray spectrum simulation for electron microprobe analysis, Microsc. Microanal. 7 (2001) 341–355.
[77] G. Castellano, J. Osán, J. Trincavelli, Analytical model for the bremsstrahlung spectrum in the 0.25–20 keV photon energy range, Spectrochim. Acta Part B 59 (2004) 313–319.
[78] T. Rao-Sahib, D. Wittry, in: G. Shinoda, K. Kohra, T. Ichinokawa (Eds.), Proc. of the 6th Intl. Conf. on X-Ray Optics and Microanalysis, Univ. of Tokyo, Tokyo, 1972, pp. 131–137.
[79] R. Packwood, J. Brown, A Gaussian expression to describe $\phi(\rho Z)$ curves for quantitative electron probe microanalysis, X-Ray Spectrom. 10 (1981) 138–145.
[80] J. Riveros, G. Castellano, J. Trincavelli, Comparison of $\phi(\rho Z)$ curves in EPMA, Mikrochim. Acta [Suppl.] 12 (1992) 99–105.
[81] K. Heinrich, Mass absorption coefficients for electron probe microanalysis, in: J. Brown, R. Packwood (Eds.), 11th Intl. Congress on X-Ray Optics and Microanalysis (ICXOM-11), University of Western Ontario, London, 1987, pp. 67–119, Canada.
[82] P. Statham, A ZAF procedure for microprobe analysis based on measurement of peak-to-background ratios, in: D. Newbury (Ed.), Microbeam Analysis, San Francisco Press, San Francisco, CA, 1979, pp. 247–253.
[83] G. Love, M. Cox, V. Scott, A versatile atomic number correction for electron-probe microanalysis, J. Phys. D 11 (1978) 7–21.
[84] A. Markowicz, R. Van Grieken, Composition dependence of bremsstrahlung background in electron-probe X-ray microanalysis, Anal. Chem. 56 (1984) 2049–2051.
[85] P. Duncumb, P. Statham, Benefits of X-ray spectrum simulation at low energies, Mikrochim. Acta 138 (2002) 249–258.
[86] J. Trincavelli, S. Limandri, A. Carreras, R. Bonetto, Experimental method to determine the absolute efficiency curves of a wavelength-dispersive spectrometer, Microsc. Microanal. (in press).
[87] S. Limandri, C. Visñovezky, A. Carreras, R. Bonetto, J. Trincavelli, Estudio de probabilidades de transición radiativa hacia las capas M en Pb, Bi, Th y U, presented at the X Latin-American Seminar on X-Ray Analytical Techniques (2006) Arica, Chile.